frontiers | Frontiers in Earth Science

ORIGINAL RESEARCH
published: 20 June 2022
doi: 10.3389/feart.2022.909749

Seasonal Variations of Chemical Weathering and CO_2 Consumption Processes in the Headwater (Datong River Basin) of the Yellow River Draining the Tibetan Plateau

Liu Yang[1,2], Fei Zhang[1,3], Yadan Hu[1], Yun Zhan[4], Li Deng[1], Huayu Huang[2]*, Hui Sun[1], Yaben Wei[4] and Xiangliang Li[5]*

[1]SKLLQG, Institute of Earth Environment, Chinese Academy of Sciences, Xi'an, China, [2]Shaanxi Key Laboratory of Earth Surface System and Environmental Carrying Capacity, College of Urban and Environmental Science, Northwest University, Xi'an, China, [3]CAS Center for Excellence in Quaternary Science and Global Change, Xi'an, China, [4]Zhengzhou Technology and Business University, Zhengzhou, China, [5]China Xi'an Satellite Control Center, Xi'an, China

The Yellow River basin covers contrasting tectonics, climate, and vegetation settings. To explore the seasonal chemical weathering differences from the upstream to downstream of the Yellow River basin, we collected weekly river waters from the Datong River draining the Tibetan Plateau in 2017. Our results show remarkably seasonal variations of major ions. A forward model was employed to quantify the contribution of silicate, carbonate, and sulfide oxidation/evaporite and atmospheric input to the cations, which yielded the contributions of 9.21 ± 1.57%, 46.07 ± 1.4%, 21.46 ± 1.03%, and 23.26 ± 1.72%, respectively, indicating a dominated carbonate weathering to the river chemistry. The significant correlation between the carbonate weathering rate and runoff suggests a critical runoff control on chemical weathering in the Datong River catchment. A comprehensive comparison between the upper and middle-lower reaches of the Yellow River basin shows a declined silicate weathering and CO_2 consumption rate ($ØCO_{2sil}$) from the upstream to downstream. In contrast, the physical erosion rate shows an increased trend, with the most prominent increase in the midstream Loess Plateau. A further comparison between the Yellow River draining the Tibetan Plateau and the Loess Plateau shows 4.5 times higher $ØCO_{2sil}$ but 9.5 times lower erosion rate. In conclusion, we propose that the runoff, rather than erosion, plays a central role on chemical weathering in the Yellow River basin, which provides insight for in-depth understanding the surficial weathering and the global carbon cycle.

Keywords: seasonal variations, Yellow River, chemical weathering, CO_2 consumption, physical erosion

OPEN ACCESS

Edited by:
Shiming Wan,
Institute of Oceanology (CAS), China

Reviewed by:
Wenjing Liu,
Institute of Geology and Geophysics (CAS), China
Santosh Kumar Rai,
Wadia Institute of Himalayan Geology, India

***Correspondence:**
Fei Zhang
zhangfei@ieecas.cn
Huayu Huang
huanghy@nwu.edu.cn

Specialty section:
This article was submitted to Hydrosphere, a section of the journal Frontiers in Earth Science

Received: *31 March 2022*
Accepted: *04 May 2022*
Published: *20 June 2022*

Citation:
Yang L, Zhang F, Hu Y, Zhan Y, Deng L, Huang H, Sun H, Wei Y and Li X (2022) Seasonal Variations of Chemical Weathering and CO_2 Consumption Processes in the Headwater (Datong River Basin) of the Yellow River Draining the Tibetan Plateau. Front. Earth Sci. 10:909749. doi: 10.3389/feart.2022.909749

1 INTRODUCTION

Chemical weathering is thought to be a major process for controlling the evolution of the Earth's surface and regulating the atmospheric CO_2 level over geological time scale (e.g., Gaillardet and Galy, 2008; Liu et al., 2018). The classical "tectonic uplift" hypothesis proposed that mountain uplift enhanced continental denudation and silicate weathering, resulting in rapidly atmospheric CO_2 drawdown and thus the Cenozoic cooling (Raymo et al., 1988; Raymo and Ruddiman, 1992). This has stimulated numerous studies to investigate the control mechanism of chemical weathering processes during the past decades (White and Blum, 1995; Gaillardet et al., 1999; Berner, 2001; Millot et al., 2002; Bickle et al., 2003; Dupré et al., 2003; Millot et al., 2003; Oliva et al., 2003; West et al., 2005; Tipper et al., 2006; Moon et al., 2007; West, 2012; Zhang et al., 2013a; Zhang et al., 2013b; Torres et al., 2014; Bickle et al., 2018; Gaillardet et al., 2019; Tipper et al., 2021). However, understanding how this process has varied in the past and what has controlled it (e.g., through changes in climatic or tectonic forcing) remains a major challenge (Willenbring and von Blanckenburg, 2010; Caves et al., 2016; Caves et al., 2019; Si and Rosenthal, 2019; Lenard et al., 2020; Clift and Jonell, 2021; Li et al., 2021).

The Yellow River, the fifth longest river in the world and the second largest in China by both length (5,464 km) and basin area (752,400 km^2), is famous for its extremely high sediment load (Milliman and Farnsworth, 2011). The sediment flux transported to the oceans has been previously estimated to be up to $1{,}100 \times 10^6$ t/yr, accompanying a solute flux of ~21×10^3 t/yr (Milliman and Farnsworth, 2011). This river originates from the Qinghai–Tibet Plateau (QTP), drains through the Loess Plateau (LP) at middle reaches, and finally flows through the downstream floodplain into the ocean. The contrasting climates, vegetations, and geomorphic settings between the tectonically active QTP and the erodible LP provide ideal conditions for in-depth understanding the weathering process under different climate and tectonic backgrounds.

Previous studies have investigated the river water chemistry and weathering processes of the Yellow River. For example, Hu et al. (1982) first reported that the solute chemistry of the Yellow River was affected by evaporites and silicate weathering and carbonate precipitation. Then, Zhang et al. (1995) conducted a detailed research and proposed that chemical weathering is the primary control of river chemistry. In the following decades, various methods, such as trace elemental and isotopic indicators, have been applied to explore the chemical weathering processes and fluxes in the Yellow River basin (e.g., Wu et al., 2005; Fan et al., 2014; Ran et al., 2015; Zhang et al., 2015; Wang et al., 2016; Li et al., 2020; Qu et al., 2020; Chai et al., 2021). Among them, most are one-time spatial sampling during flood seasons. As seasonal chemical compositions of river waters could be quite different (e.g., Zhang et al., 2013a; Ran et al., 2015), previous studies warned that estimates of weathering and CO_2 consumption rates could be biased by sampling at rain and/or dry seasons only, or missing details from extreme storm events (Zhang et al., 2015). Moon et al. (2014) also suggested that at least 10 time-series seasonal data with synchronous discharge are necessary to reduce the uncertainties of silicate weathering estimates. Till now, there are only four sets of time-series sampling (three at the Loess Plateau and one at the lower reach) in the Yellow River at the middle-lower reaches (Ran et al., 2015; Zhang et al., 2015). However, such a seasonal study of the weathering process in the upstream of the Yellow River draining the QTP, supplying for 80% of the total TDS flux for the mouth of the Yellow River (Wu et al., 2005), is still lacking, which prevents the accurate estimation of the chemical weathering flux and CO_2 consumption rate in the tectonically active QTP.

To better understand the seasonal weathering process and its sensitivity to hydrological change in the upstream Yellow River, we conducted weekly sampling in the Datong River during the whole 2017 at the Qingshizui hydrological station. The Datong River is a major tributary of the upstream Yellow River. It originates from the Qilian Mountains, northeastern of the QTP. The pristine watershed has not been affected by human activities. This study investigated seasonal chemical compositions of river waters, quantified the relative contribution of different sources to the water solutes, and estimated chemical weathering and the CO_2 consumption rate of the Datong River. Finally, we compared time-series river water chemistry and weathering processes between the upper and middle-lower reaches of the Yellow River to reveal the weathering differences in the entire Yellow River basin.

2 GEOGRAPHIC AND GEOLOGICAL BACKGROUND

The Datong River basin is located at the upstream of the Yellow River (between 98°30′ to 105°15′E and 36°30′ to 38°25′N), northeastern QTP (**Figure 1**). The elevation of the Datong basin is high in the northwest and low in the southeast with more than 80% of the basin >3,000 m. The drainage basin is bonded by two NW-SE mountains with the Datong Mountain at the south and the Tuolai Mountain at the north. The Datong River basin is a tectonic denudation mountainous area with hilly glacier accumulation platforms and alluvial plains. The total length of the Datong River is 560 km. The sampling site in this study is located in the upstream of the Datong River at the Qingshizui hydrological station, which covers a catchment area of 8,011 km^2 and a river length of 310 km.

The study area belongs to the typical plateau continental climate and is affected by the Asian summer monsoon and the winter monsoon. The climate is characterized by cold, long winter, and short summer. According to the data of the Qingshizui hydrological station, the precipitation mainly occurs from May to September (summer), accounting for 85%–92% of the annual precipitation. The total annual

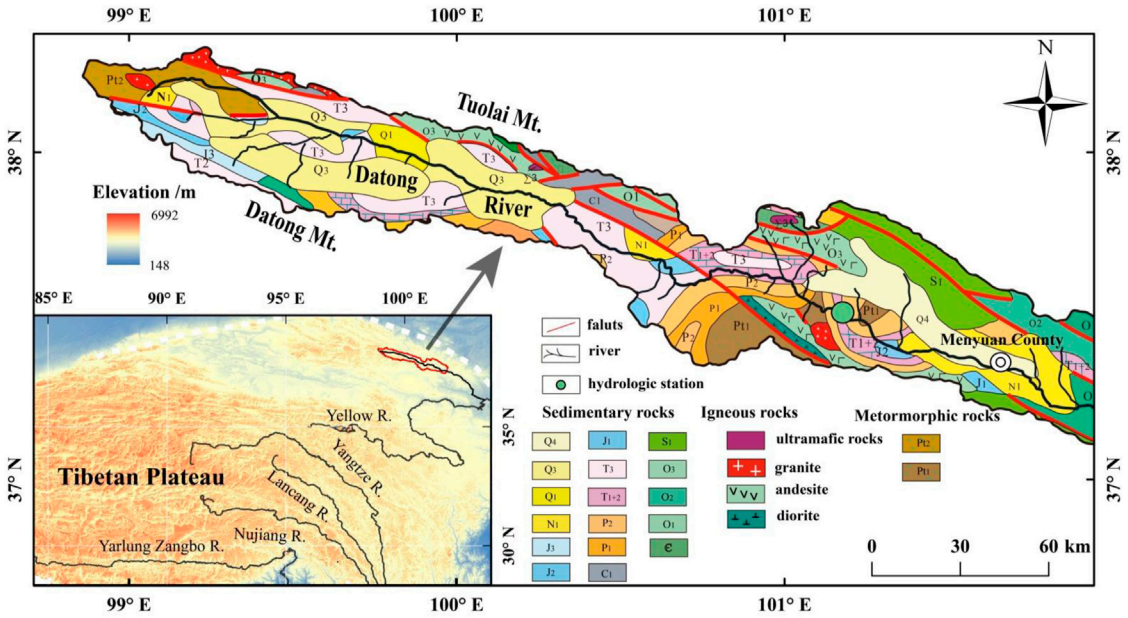

FIGURE 1 | Geological map and location of the Datong River basin at the upper reach of the Yellow River. The green cycle is the weekly sampling site of river waters in the Datong River at the Qingshizui hydrological station.

runoff of the Datong River is 293 mm. The discharge is high from June to September, accounting for >80% of the annual discharge.

The Datong River is dominated by sedimentary rocks, mainly composed of marine and terrestrial clastics, carbonates, and unconsolidated sediments, with minor volcanic and metamorphic rocks. Quartz sandstone, siltstone, calcareous siltstone, and coal seams are exposed in the study area. Limestone and dolomite are distributed in the south bank tributaries, and sandstone, mudstone, and coal seams are distributed in the north bank tributaries.

3 SAMPLES AND ANALYSIS

A total of 48 river water samples were collected weekly in the Datong River at the Qingshizui hydrological station from January to December 2017. Five rainwater samples were collected during the monsoon season in 2016. Water temperature, pH, electrical conductibility (EC), and total dissolved solids (TDS) were measured in situ by HANNA HI98129. Suspended particle matter (SPM) concentration, river water discharge (Q), precipitation (P), and water temperature (T) were monitored daily at the hydrology station.

Water samples were filtered in situ on collection through 0.45 μm Whatman® nylon filters. For cation analysis, 60 mL filtered samples were stored in precleaned polyethylene bottles and acidified to pH < 2 with 6 M distilled HNO_3. For anion measurement, 30 mL filtered samples were stored in polyethylene bottles. Each sample bottle cap is wrapped with a sealing film to prevent leakage. All samples were kept chilled at 4°C until analysis.

Major cations (Ca^{2+}, Mg^{2+}, Na^{+}, K^{+}, Sr^{2+}, and SiO_2) were analyzed by Inductively Coupled Plasma Optical Emission Spectrometer (ICP-OES) with the average reproducibility of 1%–2%, and major anions (F^{-}, Cl^{-}, NO_3^{-}, and SO_4^{2-}) were determined by the 940 professional IC with the precision <0.1%. The above measurements were conducted at the Institute of Earth Environment, Chinese Academy of Sciences (IEECAS). DIC concentration was calculated through ionic discharge balance. Five samples (QSZ16-34, QSZ16-47, QSZ16-55, QSZ16-69, and QSZ16-75) were randomly selected and titrated by the Meck alkalinity test suite with the precision of 0.05 mM to examine the validity of the calculated DIC results. Both methods produced consistent results with a relative deviation <5%.

4 RESULTS

4.1 Hydrochemical Parameter Variations

The pH, water temperature, EC, precipitations, discharges, and major ion concentrations of water samples in the Datong River are summed in **Table 1**. The water temperature varied from 1.8 to 17.1°C, with an average of 8.30 ± 4.28°C (**Figure 2**). The pH and EC ranged from 7.89 to 8.77 with an average of 8.26 ± 0.21, and from 320 to 390 μS/cm with an average of 363 ± 18 μS/cm, respectively. The maximum discharge of 117 m^3/s occurred in June, and the mean daily discharge for the entire year was 73 m^3/s. The discharge can be divided into two regimes that

TABLE 1 | Physico-chemical parameters and major ion concentrations of river water in the Datong River.

Sample no.	Date	T_w (°C)	pH	EC μs/cm	Ca^{2+}	Mg^{2+}	Na^+	K^+	Si	HCO_3^-	SO_4^{2-}	Cl^-	NO_3^-
					μmol/L								
QSZ16-29	2017/1/2	2.40	8.42	360	1,397	737	551	50.8	162	3,449	623	156	40.1
QSZ16-30	2017/1/6	4.10	9.43	350	1,396	736	552	49.6	155	3,433	630	158	35.8
QSZ16-31	2017/1/13	3.50	8.45	350	1,371	711	525	47.0	154	3,313	624	156	39.6
QSZ16-32	2017/1/20	3.00	8.12	350	1,392	734	547	49.1	155	3,403	633	158	43.0
QSZ16-33	2017/1/28	4.30	8.12	350	1,391	728	539	50.0	158	3,373	634	160	45.4
QSZ16-34	2017/2/5	3.40	8.45	360	1,403	730	534	48.2	159	3,385	638	160	46.8
QSZ16-35	2017/2/12	4.50	8.29	360	1,413	744	549	49.1	160	3,432	645	163	46.9
QSZ16-36	2017/2/19	3.80	8.27	370	1,411	755	550	49.1	162	3,442	650	164	48.1
QSZ16-37	2017/2/26	3.50	8.30	370	1,436	766	553	50.1	163	3,507	653	167	47.8
QSZ16-38	2017/3/6	4.60	8.39	390	1,424	759	546	48.3	160	3,448	659	169	48.3
QSZ16-39	2017/3/12	4.30	8.09	390	1,443	776	557	50.2	165	3,535	657	169	48.8
QSZ16-40	2017/3/19	4.60	8.15	390	1,464	787	562	49.9	167	3,587	664	171	49.1
QSZ16-41	2017/3/29	3.60	8.52	370	1,484	802	582	52.6	171	3,699	655	170	49.0
QSZ16-42	2017/4/2	6.30	8.05	380	1,504	813	590	52.7	173	3,764	659	171	47.4
QSZ16-43	2017/4/9	7.40	8.14	390	1,478	817	569	50.3	172	3,674	666	177	49.4
QSZ16-44	2017/4/16	5.30	8.45	390	1,468	800	567	51.5	170	3,625	664	175	49.9
QSZ16-45	2017/4/23	7.00	8.22	360	1,456	789	562	52.0	169	3,594	655	174	48.7
QSZ16-46	2017/4/29	9.30	8.44	380	1,451	788	549	49.2	166	3,550	662	177	48.6
QSZ16-47	2017/5/7	8.20	8.40	370	1,435	766	540	48.9	165	3,496	647	173	48.3
QSZ16-48	2017/5/13	7.70	8.30	370	1,433	776	545	49.3	169	3,511	651	175	47.3
QSZ16-50	2017/5/26	9.30	8.30	370	1,365	738	510	44.9	162	3,295	627	184	48.0
QSZ16-51	2017/6/1	10.6	8.38	360	1,351	711	497	45.9	158	3,232	619	171	46.9
QSZ16-52	2017/60/8	10.6	8.70	360	1,338	721	506	44.4	157	3,225	618	181	47.0
QSZ16-53	2017/6/16	12.5	8.18	360	1,315	697	486	43.0	155	3,140	604	177	45.2
QSZ16-54	2017/6/24	12.6	7.91	360	1,311	698	488	41.6	155	3,143	601	181	45.6
QSZ16-55	2017/7/02	12.0	8.04	350	1,286	680	467	42.0	154	3,061	586	180	44.3
QSZ16-56	2017/7/11	15.7	8.05	360	1,288	678	482	42.2	148	3,108	574	177	44.3
QSZ16-57	2017/7/21	15.3	7.97	330	1,292	690	480	41.5	153	3,115	584	179	41.4
QSZ16-58	2017/7/28	15.8	8.01	330	1,211	633	443	41.4	140	2,917	537	158	42.5
QSZ16-59	2017/8/10	16.0	7.93	320	1,186	615	425	40.7	138	2,814	538	152	41.4
QSZ16-60	2017/8/20	17.1	8.00	330	1,171	604	415	43.4	137	2,785	524	149	41.1
QSZ16-61	2017/8/28	13.2	8.07	330	1,208	621	439	42.4	143	2,911	529	146	41.7
QSZ16-62	2017/9/04	13.5	7.94	340	1,207	614	436	44.5	142	2,847	554	141	47.4
QSZ16-63	2017/9/11	12.3	8.12	340	1,237	629	438	41.5	145	2,875	583	142	46.2
QSZ16-64	2017/9/17	11.9	8.33	350	1,228	617	422	40.4	145	2,773	607	135	45.5
QSZ16-65	2017/9/25	11.5	8.28	350	1,262	642	442	41.7	147	2,905	611	137	45.4
QSZ16-66	2017/10/2	12.1	7.89	360	1,284	663	457	46.3	161	3,013	608	142	47.0
QSZ16-67	2017/10/9	11.2	8.47	360	1,278	656	447	45.9	165	2,944	619	148	49.0
QSZ16-68	2017/10/18	10.2	8.07	380	1,297	674	467	45.9	159	3,014	631	151	47.1
QSZ16-69	2017/10/26	10.5	8.24	360	1,298	671	462	41.2	147	2,974	647	149	45.4
QSZ16-70	2017/11/03	8.10	8.45	370	1,344	696	478	42.8	152	3,112	656	151	46.0
QSZ16-71	2017/11/09	6.90	8.23	380	1,362	711	498	44.6	155	3,188	660	155	46.3
QSZ16-72	2017/11/17	7.60	8.77	390	1,357	720	498	43.5	153	3,165	670	163	47.1
QSZ16-73	2017/11/25	6.60	8.43	390	1,383	745	517	44.9	161	3,284	670	167	48.6
QSZ16-74	2017/12/02	3.40	8.47	380	1,388	756	521	45.5	176	3,319	672	168	45.3
QSZ16-75	2017/12/09	5.10	8.17	380	1,359	727	494	43.0	154	3,174	670	167	47.2
QSZ16-76	2017/12/16	1.80	8.53	370	1,368	735	500	45.7	154	3,191	683	167	47.4
QSZ16-77	2017/12/25	4.30	8.49	370	1,368	743	511	43.5	153	3,217	686	167	41.3

T_w: water temperature.

correspond to the monsoon climate: low-flow (October to May) and high-flow (June to September).

The total cationic charge ($TZ^+ = Na^+ + 2Ca^{2+} + 2Mg^{2+} + K^+$) varied from 4,005 to 5,276 μEq, much higher than the world average of ~1,250 μEq/L (Meybeck, 1979). The total molar cation concentrations follow an order of $Ca^{2+} > Na^+ > Mg^{2+} > K^+$ in the Datong River catchment. As shown in the ternary diagram (**Figure 3**), the major cation is Ca^{2+}, with an average of 1,354 μM, contributing to ~60% of TZ^+, and the second is Na^+, accounting for ~30% of TZ^+. The total anionic charge ($TZ^- = HCO_3^- + Cl^- + 2SO_4^{2-} + NO_3^- + F^-$) varied from 4,028 to 5,500 μEq. The molar anion concentrations follow an order of $HCO_3^- > SO_4^{2-} > Cl^- > NO_3^- > F^-$. Among them, HCO_3^- had an average of 3,249 μM, accounting for 70% of the TZ^- in charge equivalent units (**Figure 3**).

4.2 Seasonal Variations of Major Ions in River Waters

All the physico-chemical parameters presented clear seasonal variations in the Datong River catchment (**Figure 2**).

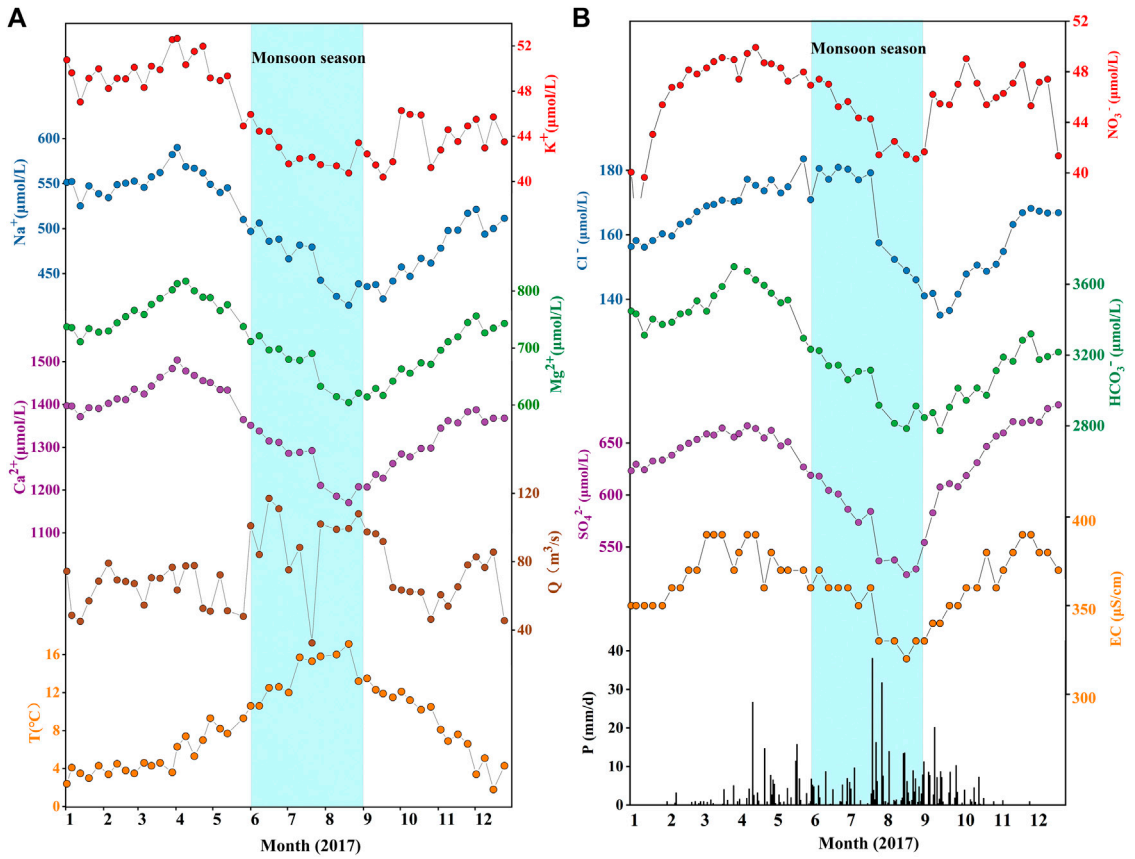

FIGURE 2 | Weekly variations of **(A)** major cations, **(B)** major anions and hydrometeorological data in the Datong River monitored at the Qingshizui hydrological station in 2017. **(A)** Shows the seasonal changes of main cations, water temperature and runoff in the river, and **(B)** shows the seasonal changes of main anions, conductivity and precipitation in the river. The major ions show clear seasonal variations, with low values in rainy season and high values in dry season. The sky blue bars mark the monsoon season.

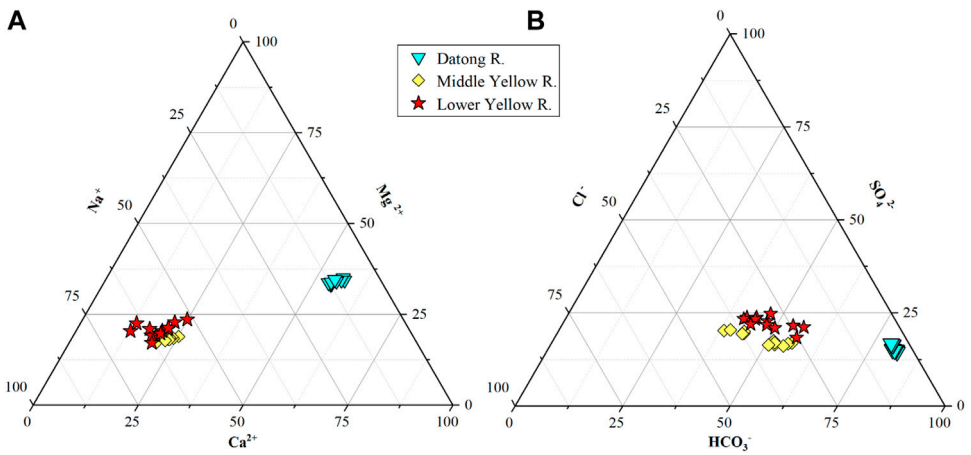

FIGURE 3 | Proportion of **(A)** major cations **(B)** major anions in river water of the Datong River basin. The middle reaches data (Longmen) come from Zhang et al. (2015) and the downstream data (Lijin) come from Ran et al. (2015).

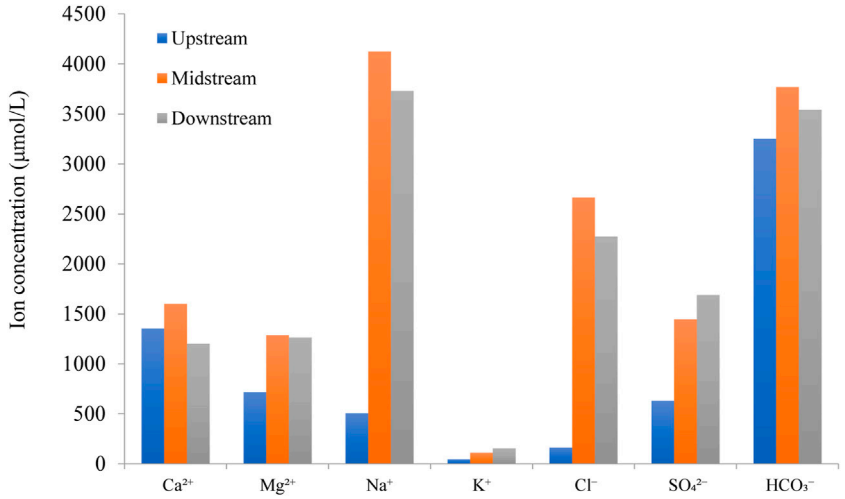

FIGURE 4 | Comparison of the major ion concentration in the upper, middle, and lower reaches of the Yellow River. The major ion concentrations are the average of river waters collected weekly in the upstream (this study), midstream (Longmen), and downstream (Lijin). The midstream and downstream data come from Zhang et al. (2015) and Ran et al. (2015), respectively.

Precipitation mainly occurred from late April to October in 2017. Previous studies in surrounding catchments reported several orders of magnitude changes of seasonal river discharge (Zhang et al., 2013a). However, in this study, river discharge only showed a slight increase (~3-fold) from dry to flood seasons and did not show a synchronous variation with precipitation, which can be attributed to the damming effect at the upstream of the Qingshizui hydrological station. The water temperature rose from January to the peak in August and then declined to the lowest in December. The major ion concentrations were systematically lower in rainy season and higher in dry season, opposite to the trend of the water temperature. Although major ions displayed similar seasonal variations, minor differences still existed, e.g., the concentrations of K^+, Na^+, Mg^{2+}, Ca^{2+}, HCO_3^-, and SO_4^{2-} slightly increased from January to early April and then rapidly declined with increasing monsoonal rainfall. The concentration of NO_3^- increased sharply from January to April, but its minimum value appeared in January rather than in August as other ions. Overall, the similarities of the seasonal variations of ions reflect the dilution effect of precipitation in rainy season.

4.3 Seasonal Differences of Major Ions Between the Upper vs. Middle to Lower Reaches of the Yellow River

Spatially, there are two typical characters of river water chemistry between the upper vs. middle to lower reaches of the Yellow River (**Figure 4**). 1) All major ion concentrations (excluding Ca^{2+}) in the upper reach (Datong River) were lower than the middle (Longmen) to lower reaches (Lijin) of the Yellow River, while the concentrations in the midstream were comparable with the downstream. 2) The Na^+, Cl^-, and SO_4^{2-} in the middle to lower reaches were significantly higher than that of the upper reach of the Yellow River, for which the Na^+ and Cl^- are 8 × and 16 × higher in the middle relative to the upper reaches. These extremely high concentrations suggest an important contribution of evaporite dissolution during weathering in the Loess Plateau. The spatial differences and evaporite contribution can also be observed in **Figure 3**.

Seasonally, we further selected the weekly data of the Datong River in the upper reach and the Longmen station in the middle reach for comparison to reveal their differences (**Figure 5**). The major similarities are as follows: 1) The overall seasonal variations pattern is similar, showing lower ion concentrations during the monsoonal period, and higher values during the dry seasons. 2) As pointed out by Zhang et al. (2015) that there was a snow/ice melting imprint during spring seasons (around April) in the middle reach of the Yellow River at the Longmen station, the imprint can also be identified in the upstream Datong River. This is supported by the first peak of the water discharge during March to April in the Longmen station. Importantly, the consistent melting fingerprint indicates that the melting signal can be directly propagated to the middle reaches of the Yellow River, implying the significant contribution of water discharge from the upstream Tibetan Plateau to the downstream in dry season. Obviously, the large ice/glacier reservoir exists in the Tibetan Plateau, rather than in the Loess plateau. In addition, the increasing ion concentrations during the melting period in the Datong River is also helpful to explain the observed pulse-type increase of ion contents in the downstream Longmen station. Here, we think the increased ion concentration in the Datong River most likely reflect the salt-contained dust deposition during frequently spring dust-storm events (Jin et al., 2011).

There is also a clear difference between the upper and middle reaches (**Figure 5**). During the flood season (July to September),

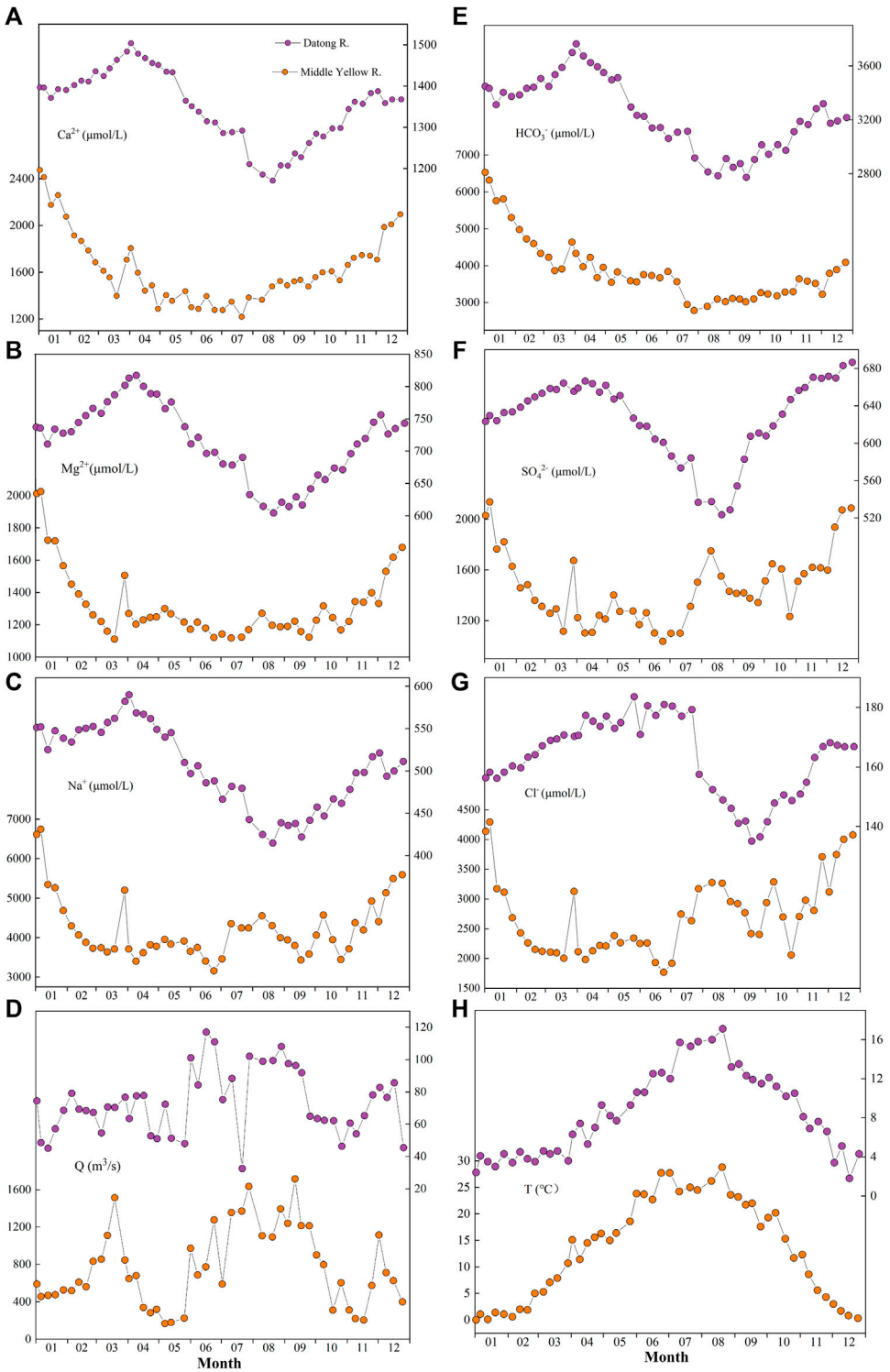

FIGURE 5 | Comparisons of seasonal variations of **(A)** Ca^{2+}, **(B)** Mg^{2+}, **(C)** Na^{+}, **(D)** Runoff, **(E)** HCO^{3-} **(F)** SO^{42-}, **(G)** Cl^{-}, and **(H)** Water temperature between the upstream and midstream of the Yellow River. The time-series data of the upstream (purple) are the Datong River (this study). The weekly data of the midstream (orange) are from Zhang et al. (2015).

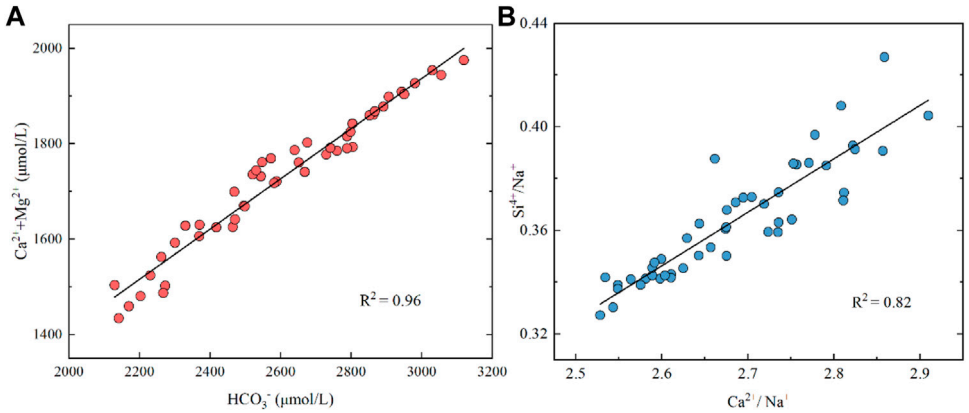

FIGURE 6 | Plot of $Ca^{2+}+Mg^{2+}$ versus HCO_3^- and Si^{4+}/Na^+ versus $Ca^{2+}+Na^+$ of river water in the Datong River. The data suggest potential carbonate and silicate weathering in the Datong River catchment.

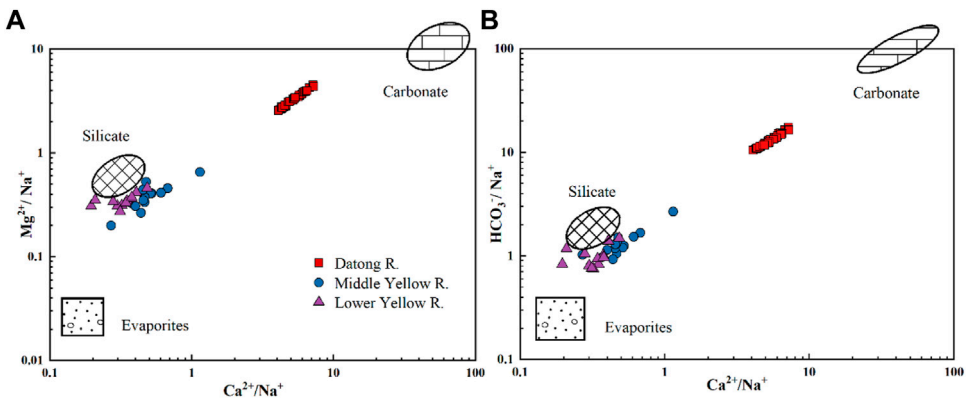

FIGURE 7 | Elemental ratios of Ca^{2+}/Na^+ vs. Mg^{2+}/Na^+ and Ca^{2+}/Na^+ vs. HCO_3^-/Na^+ of river water in the Datong River. The endmember values are from Gaillardet et al. (1999). The middle reaches data (Longmen) come from Zhang et al. (2015). The downstream data (Lijin) come from Ran et al. (2015).

TABLE 2 | Concentrations of major ions in rain waters collected from the Datong River catchment in 2016.

Sample no.	Date	Na^+	K^+	Ca^{2+}	Mg^{2+}	Cl^-	NO_3^-	SO_4^{2-}	HCO_3^-
		μmol/L							
YS16-1	2016/6/20	272	181	206	58.5	12.5	21.2	5.50	875
YS16-2	2016/6/21	59.2	27.6	110	13.3	14.4	249	14.8	39.1
YS16-3	2016/6/26	104	29.7	148	20.8	24.8	44.4	26.3	283
YS16-4	2016/7/25	263	36.2	222	26.7	15.1	344	26.6	382
YS16-5	2016/8/26	59.6	58.2	60	19.2	36.9	27.4	8.90	88.5

all the ion concentration in the upstream and midstream was diluted to the lowest, but it is interesting to find that unlike the upstream, the concentration of Na^+, Cl^-, and SO^{2-4} in the midstream Longmen began to increase (**Figures 5C,F,G**), indicating the fast dissolution of evaporite during the rainy season in the Loess Plateau. This reflects their distinct control mechanisms of weathering processes between the upper and middle reaches of the Yellow River.

5 DISCUSSION

5.1 Sources of Dissolved Loads in the Datong River

The dissolved loads of river water are generally affected by natural (e.g., atmospheric inputs and chemical weathering) and anthropogenic activity (Roy et al., 1999; Moon et al., 2007; Moquet et al., 2011). In this study, damming at the upstream

of the Datong River may significantly alter the river discharge. However, weekly major ions show clear seasonal variations with dilution effects by monsoonal rainfall, implying that damming has limited impacts on seasonal variations of water chemistry in the Datong River. Due to the sparse population, the input of human activities to river chemistry could be negligible. This is supported by the very low weekly NO_3^-concentrations (<50 μmol/L), which is comparable with other regions in the QTP that suggested a minor influence from anthropogenic input, e.g., the Jinsha River and Yarlung Tsangpo River (Zhang et al., 2016; Qu et al., 2017).

Globally, river hydrochemistry is commonly affected by carbonate weathering, which mainly supplies Ca^{2+}, Mg^{2+}, and HCO_3^- to the dissolved load (Gaillardet et al., 2019). The dominance of HCO_3^- and Ca^{2+} in the Datong River, together with their higher concentrations than other QTP-originated rivers draining basalt and granite lithology, such as the Min River (960 μM, 1,970 μM) and Jinsha River (931 μM, 2,066 μM) (Zhong et al., 2017), indicates that carbonate weathering may have occurred in the watershed. This is consistent with the significant correlation (r^2 = 0.95) between (Ca^{2+} + Mg^{2+}) and HCO_3^- (**Figure 6A**).

Evaporite dissolution has been proposed to play an important role in arid and semi-arid regions (Fan et al., 2014). Halite dissolution could release Na^+ and Cl^- to river water at 1:1 stoichiometry. However, no evaporite exposed in the watershed (**Figure 1**) suggests that halite dissolution seems not to be a major factor in controlling the weathering in this region, in particular when considering the very high contents of Na^+ and Cl^- in the middle to lower reaches of the Yellow River. Si is generally derived from silicate weathering. The good correlation between Ca^{2+}/Na^+ and Si/Na^+ (r^2 = 0.82) (**Figure 6B**) indicates that silicate weathering is another player in weathering processes in the QTP river basin. The carbonate and silicate weathering in the upstream Datong River catchment is also observed by element ratios, showing the data points between carbonate and silicate endmembers (e.g., Ca/Na vs. Mg/Na, **Figure 7**).

5.2 Forward Model Calculations

5.2.1 Atmospheric Input

Atmospheric deposition is one of the sources for ions in river (Liu et al., 2016a; Liu et al., 2016b). The purpose of correcting atmospheric input is to quantify the contribution of rainwater to the chemical composition of river water. We collected five rainwater samples (**Table 2**) in the study area and followed the calibration method of Grosbois et al. (2000):

$$X^* = (X/Cl)_{rain} \times Cl_{ref}, \quad (1)$$

where X^* refers to the corrected concentration derived from rainwater, $(X/Cl)_{rain}$ refers to the measured ion/ Cl in rain water, and Cl_{ref} is the Cl^- concentration in river water derived from rainwater,

$$Cl_{ref} = F \times Cl_{ave}, \quad (2)$$

where Cl_{ave} is the weighted mean of the Cl^- concentration in rain samples and F is a correction factor and calculated as follows:

$$F = P/(P - E), \quad (3)$$

where P is the annual precipitation (in mm) and E is the annual evapotranspiration (in mm).

According to the 2017 hydrological data monitored by the Qingshizui hydrological station, the annual rainfall of the Datong River is 557 mm, and the annual discharge is 293 mm (P-E). The calculated F value is 1.9. The quantified result shows that the contribution of rainwater to the dissolved load of the Datong River is 20.2%–27.5% and increases with the runoff, indicating the non-negligible atmospheric contribution to the river water.

5.2.2 Rock Weathering

Weathering of silicates can contribute Na^+, K^+, Ca^{2+} and Mg^{2+} to the dissolved load. The contribution of silicate weathering to river water cations is as follows:

$$Na_{sil} = Na_{river} - Na_{rain} - Na_{halit}, \quad (4)$$

$$Na_{halit} = Cl_{halit} - Cl_{river} - Cl_{rain}, \quad (5)$$

$$K_{sil} \simeq K_{riv}, \quad (6)$$

$$Ca_{sil} = Na_{sil} \times (Ca/Na)_{sil}, \quad (7)$$

$$Mg_{sil} = Na_{sil} \times (Mg/Na)_{sil}, \quad (8)$$

where $(Ca^{2+}/Na^+)_{sil}$ and $(Mg^{2+}/Na^+)_{sil}$ are the molar ratios released to river water from silicates during weathering. The $(Ca^{2+}/Na^+)_{sil}$ and $(Mg^{2+}/Na^+)_{sil}$ in this study are 0.35 and 0.24, respectively, based on the data from Gaillardet et al. (1999). The calculated results show that contributions of silicate weathering range from 6.1 to 11.9%, with an average of 9.2% in the Datong River catchment. Among them, the silicate contribution in the dry period (January–May and October–December) is 9.74%, higher than the monsoon period (June–September) of 7.45%, which is consistent with the previous studies (Zhang et al., 2015; Yu et al., 2019). The lower contribution in the monsoonal season reflects short water–rock reaction time, which inhibits the weathering of silicate minerals (Jiang et al., 2018).

Carbonate weathering releases Ca^{2+} and Mg^{2+} to river, and the calculation for carbonate contribution is as follows:

$$Ca_{carb} = Ca_{river} - Ca_{rain} - Ca_{sil}, \quad (9)$$

$$Mg_{carb} = Mg_{river} - Mg_{rain} - Mg_{sil}. \quad (10)$$

The results show that the contributions of carbonate weathering range from 43.8 to 47.6% with an average of 46.1% (**Table 3**), indicating that carbonate weathering dominated the river chemistry in the Datong River catchment. Different from silicate weathering, the contribution of carbonate dissolution to dissolved loads is higher in the monsoon period than in the dry period. This is due to the fast carbonate dissolution dynamics relative to silicates in the rainy season (Zhang et al., 2013a; Zhang et al., 2013b; Gaillardet et al., 2019).

5.2.3 Evaporite Dissolution and Sulfide Oxidation

Evaporite weathering generally includes halite and gypsum. River water SO_4^{2-} can be derived from gypsum dissolution or oxidation

TABLE 3 | Chemical weathering fluxes and CO_2 consumption rates for the Datong River catchment.

Sample No	Date	Q	PER[a]	Rain	Silicates	Carbonates	Sul/Evp[b]	SWR[c]	CWR[d]	$ØCO_{2sil}$[e]	$ØCO_{2carb}$[f]
		m^3/s	$kg/km^2/day$	Cations %					$10^3mol/km^2/yr$		
QSZ16-29	2017/1/2	74.4	1.60	22.3	11.5	46.0	20.2	137	494	108	487
QSZ16-30	2017/1/6	48.6	6.29	22.3	11.3	45.7	20.7	87	323	70.2	318
QSZ16-31	2017/1/13	45.1	5.35	22.9	10.4	45.7	21.0	74	293	55.0	290
QSZ16-32	2017/1/20	57.1	2.46	22.4	11.1	45.6	20.9	101	378	80.0	373
QSZ16-33	2017/1/28	68.6	10.4	22.5	10.7	45.7	21.0	118	454	90.0	449
QSZ16-34	2017/2/5	79.1	9.38	22.4	10.5	46.0	21.1	133	529	100	536
QSZ16-35	2017/2/12	69.3	11.9	22.1	10.9	45.8	21.2	122	468	94.9	475
QSZ16-36	2017/2/19	68.4	15.5	22.0	10.9	45.8	21.2	121	464	94.2	471
QSZ16-37	2017/2/26	67.2	21.0	21.7	10.8	46.4	21.1	119	466	92.3	472
QSZ16-38	2017/3/6	54.6	18.8	21.9	10.4	46.1	21.6	93	375	70.5	381
QSZ16-39	2017/3/12	70.6	11.4	21.5	10.8	46.5	21.1	127	494	98.5	501
QSZ16-40	2017/3/19	70.3	7.58	21.2	10.9	46.8	21.1	129	499	100	507
QSZ16-41	2017/3/29	76.7	16.5	20.9	11.7	47.2	20.3	152	552	123	560
QSZ16-42	2017/4/2	63.4	21.9	20.6	11.9	47.5	20.1	129	463	106	469
QSZ16-43	2017/4/9	77.5	8.36	20.8	10.8	47.6	20.8	144	564	110	572
QSZ16-44	2017/4/16	77.7	5.87	21.1	10.9	47.1	20.9	144	557	111	565
QSZ16-45	2017/4/23	52.7	13.6	21.3	10.8	47.1	20.8	96	374	73.9	379
QSZ16-46	2017/4/29	51.0	18.7	21.4	10.1	47.2	21.3	87	362	64.0	367
QSZ16-47	2017/5/7	72.3	21.8	21.8	10.0	47.2	21.0	121	504	87.5	511
QSZ16-48	2017/5/13	51.3	4.98	21.7	10.2	47.1	21.0	87	359	63.6	364
QSZ16-50	2017/5/26	48.0	4.14	22.8	8.50	47.2	21.5	67	321	40.6	325
QSZ16-51	2017/6/1	101	12.0	23.3	8.60	46.8	21.3	139	659	85.5	668
QSZ16-52	2017/6/8	84.2	8.17	23.3	8.50	46.7	21.5	115	548	70.4	556
QSZ16-53	2017/6/16	117	5.05	23.9	7.90	46.8	21.4	147	745	81.1	755
QSZ16-54	2017/6/24	111	3.59	23.9	7.80	47.0	21.4	137	706	74.9	716
QSZ16-55	2017/7/2	75.2	1.62	24.5	6.90	47.4	21.3	82	469	36.6	476
QSZ16-56	2017/7/11	88.3	2.86	24.4	7.60	47.3	20.7	105	548	57.2	555
QSZ16-57	2017/7/21	32.5	0.70	24.2	7.50	47.4	21.0	38	204	19.9	207
QSZ16-58	2017/7/28	102	3.30	26.0	6.90	47.0	20.1	106	588	48.8	597
QSZ16-59	2017/8/10	98.9	1.07	26.7	6.40	46.4	20.5	94	557	36.5	565
QSZ16-60	2017/8/20	99.4	2.14	27.1	6.10	46.7	20.1	90	551	30.9	559
QSZ16-61	2017/8/28	108	15.1	26.2	7.50	46.8	19.5	119	615	59.4	623
QSZ16-62	2017/9/4	97.4	26.3	26.4	7.60	45.4	20.7	108	551	54.9	559
QSZ16-63	2017/9/11	96.3	2.08	25.8	7.60	45.1	21.6	108	561	55.1	569
QSZ16-64	2017/9/17	91.8	1.98	26.2	7.10	43.8	22.9	97	529	44.9	537
QSZ16-65	2017/9/25	64.9	2.80	25.3	7.90	44.5	22.3	77	387	42.3	392
QSZ16-66	2017/10/2	63.4	1.37	24.7	8.70	45.2	21.4	84	387	48.2	392
QSZ16-67	2017/10/9	62.4	0.67	24.9	8.00	45.0	22.1	77	380	38.4	385
QSZ16-68	2017/10/18	62.2	0.67	24.4	8.50	44.7	22.4	82	385	47.5	391
QSZ16-69	2017/10/26	46.3	0.50	24.5	8.00	44.1	23.4	57	287	33.2	291
QSZ16-70	2017/11/3	60.6	1.31	23.6	8.60	44.9	23.0	82	390	51.3	396
QSZ16-71	2017/11/9	54.0	0.58	23.2	9.20	44.9	22.7	79	352	53.3	357
QSZ16-72	2017/11/17	65.3	0.70	23.1	8.80	44.7	23.4	92	428	59.8	434
QSZ16-73	2017/11/25	78.1	0.00	22.6	9.40	45.4	22.6	120	525	82.0	532
QSZ16-74	2017/12/2	82.8	0.89	22.4	9.80	45.5	22.3	133	561	89.2	569
QSZ16-75	2017/12/9	76.6	1.65	23.1	8.40	45.2	23.3	104	506	64.3	514
QSZ16-76	2017/12/16	85.6	0.92	22.9	8.70	44.8	23.7	120	570	77.7	578
QSZ16-77	2017/12/25	45.5	0.49	22.7	9.10	44.5	23.7	66	303	45.3	308

[a]*Physical erosion rate.*
[b]*Sulfide oxidation and evaporite.*
[c]*Silicate weathering rate.*
[d]*Carbonate weathering rate.*
[e]*CO_2 consumption rate caused by silicate weathering.*
[f]*CO_2 consumption rate caused by carbonate dissolution.*

of sulfides. The weak correlation between SO_4^{2-} and Cl^- (r^2 = 0.10) indicates that the dissolution of gypsum in the Datong River basin is not a major source for river SO_4^{2-}. **Figure 7** shows that most river water samples collected in the Datong River basin are far away from the evaporite endmember. Moreover, considering the coal mining in this area, we assumed that SO_4^{2-} was mainly derived from sulfide oxidation rather than the dissolution of gypsum. Then, the rest of the weathering contribution from evaporite and oxidation of sulfides can be simply estimated as follows:

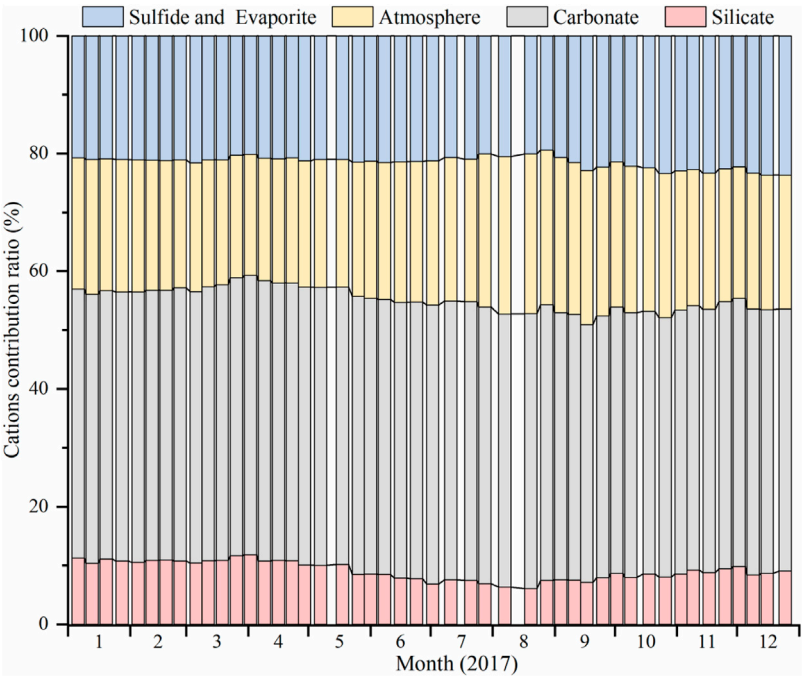

FIGURE 8 | Contribution of different sources to total cations in river water of the Datong River basin. The data show that carbonate weathering dominates the river chemistry.

TABLE 4 | Chemical weathering and CO_2 consumption rates from the upper to lower reaches of the Yellow River.

River		Area	Runoff	CWR	SWR	$ØCO_2$ *car*	$ØCO_2$ *sil*	References
		10^3km^2	mm/yr			10^5 Mol/km^2/yr		
Time-series comparison								
Upper	Datong River	8.01	293	4.71	1.05	4.76	0.69	This study
	Yellow River@Taodaoguai	368	48.3	n.a	n.a	0.61	0.38	Ran et al. (2015)
Middle	YellowRiver@Longmen	498	49.3	0.66	0.69	0.66	0.99	Zhang et al. (2015)
	YellowRiver@Tongguan	725	47.6	n.a	n.a	0.58	0.27	Ran et al. (2015)
Lower	YellowRiver@Lijin	752	36.9	n.a	n.a	0.51	0.18	Ran et al. (2015)
Spatial comparison								
Upper	Upstream (above Lanzhou)	223	170	n.a	n.a	3.04	0.14	Fan et al. (2014)
	Yellow River@Lanzhou	232	172	4.23	2.04	n.a	0.88	Wu et al. (2005)
	Taohe River	19.7	243	0.79	0.12	n.a	0.60	Wu et al. (2005)
	YellowRiver@Tangnag	123	225	3.39	0.45	n.a	0.37	Wu et al. (2005)
Middle	Midstream (Lanzhou to Huayuankou)	507	76.5	n.a	n.a	0.65	0.21	Fan et al. (2014)
	Weihe River@Main tributary	135	509	1.37	0.37	1.38	0.49	Jia et al. (2021)
Lower	Downstream (Huayuankou to river mouth)	22	395	n.a	n.a	n.a	5.62	Fan et al. (2014)
Global average	60 largest global rivers	51,098	535	n.a	n.a	2.80	2.00	Gaillardet et al. (1999)

Note. n.a denotes data not available.

$$\text{Sulfide oxidation and Evaporite\%} = 100\% - \text{Rain\%} - \text{Silicate\%} - \text{Carbonate\%}. \quad (11)$$

The contribution of sulfide oxidation and evaporite ranged from 19.5 to 23.7% with an average of 21.5%. In summary, the order of the contribution ratios of different sources to dissolved load in the Datong River is as follows: carbonate dissolution > atmospheric input ≈ sulfide oxidation and evaporite > silicate weathering (**Figure 8**).

5.3 Chemical Weathering and CO_2 Consumption Rates

5.3.1 Chemical Weathering Rate

The carbonate weathering rate (*CWR*) and silicate weathering rate (*SWR*) are calculated based on cation components derived from carbonate and silicate, drainage area, and runoff (Moon et al., 2007; Zhang et al., 2013a; Liu et al., 2018). CWR and SWR can be calculated as follows:

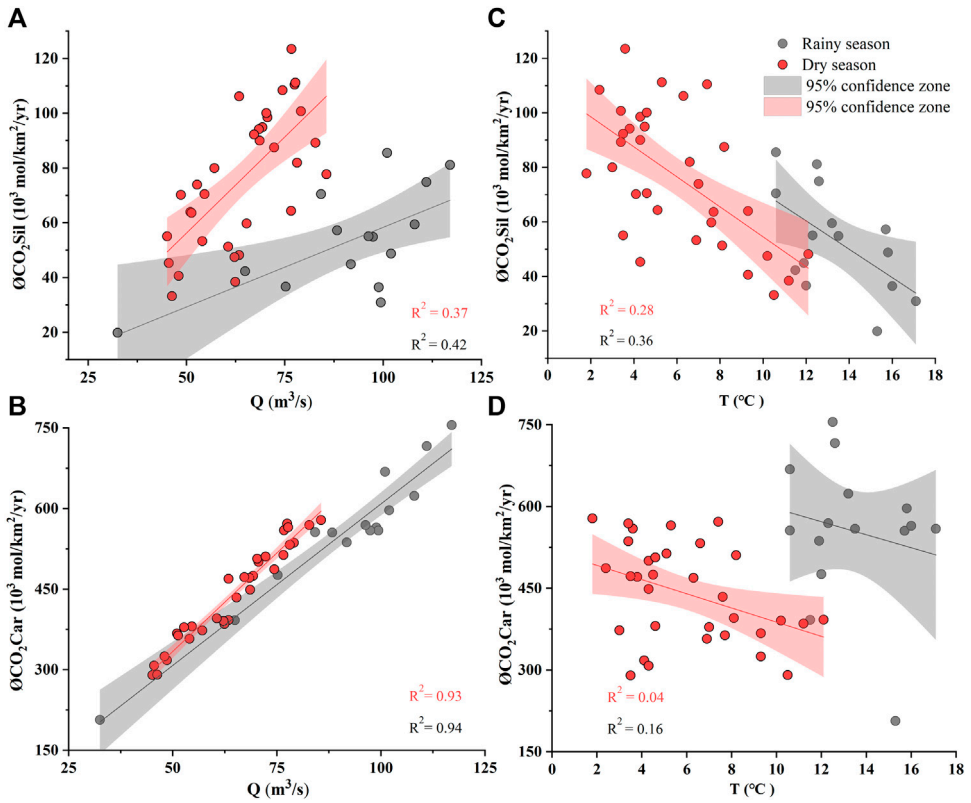

FIGURE 9 | Relationships between the CO_2 consumption rate ($ØCO_2$) and discharge and water temperature. Significant correlations are observed between $ØCO_{2car}$ and Q, indicating a critical runoff control on carbonate weathering. No clear correlations are observed between $ØCO_2$ and temperature.

$$SWR = \left([Na]_{sil} + [Ca]_{sil} + [Mg]_{sil} + [K]_{sil} + [SiO_2]_{river}\right) \times Q/A, \quad (12)$$

$$CWR = \left(2[Ca]_{carb} + 2[Mg]_{carb}\right) \times Q/A. \quad (13)$$

The calculated results showed that the *SWR* and *CWR* of the Datong River catchment ranged from 0.38 to 1.52 × 10^5 mol/km^2/yr with an average of 1.05 × 10^5 mol/km^2/yr and 2.04 to 7.45 × 10^5 mol/km^2/yr with an average of 4.71 × 10^5 mol/km^2/yr, respectively (**Table 4**).

5.3.2 Rates of CO_2 Consumption by Chemical Weathering

Assuming the sulfuric acid (H_2SO_4) generated by sulfide oxidation reacts preferentially with carbonate (Zhang et al., 2013a), the CO_2 consumption rate caused by silicate ($ØCO_{2sil}$) and carbonate weathering ($ØCO_{2carb}$) can be calculated from the flux of total dissolved cations produced by silicate and carbonate weathering, respectively:

$$ØCO_{2sil} = \left([Na]_{sil} + [K]_{sil} + 2[Ca]_{sil} + 2[Mg]_{sil}\right) \times Q/A, \quad (14)$$

$$ØCO_{2carb} = \left([Ca]_{carb} + [Mg]_{carb}\right) \times Q/A. \quad (15)$$

The CO_2 consumption rates from silicate and carbonate weathering ($ØCO_{2sil}$ and $ØCO_{2carb}$) of the Datong River catchment are 0.69 × 10^5 mol/km^2/yr and 4.76 × 10^5 mol/km^2/yr, respectively. If all H_2SO_4 generated by sulfide oxidation reacts preferentially with silicate, the $ØCO_{2sil}$ are negative.

5.3.3 Controls on Chemical Weathering Rate and $ØCO_2$

Lithology, climate (runoff/precipitation and temperature), and erosion rate are proposed to major factors that control the chemical weathering rate (Singh et al., 2005; Goldsmith et al., 2010; Zhang et al., 2019).

In the Datong River catchment, the $ØCO_{2carb}$ show significant correlations with *Q* during both rainy (r^2 = 0.94) and dry seasons (r^2 = 0.93) (**Figure 9B**), highlighting a strong control of runoff on carbonate weathering. For the $ØCO_2$ of silicate, weak positive correlations are observed between $ØCO_{2sil}$ and *Q* in both rainy and dry seasons (**Figure 9A**). In addition, no obvious correlation is observed between $ØCO_2$ and water temperature either during the rainy or dry season for both carbonate and silicate weathering (**Figures 9C,D**). Although several studies suggested an important temperature control on weathering (Dessert et al., 2005; Dixon et al., 2010), this is not the case in the Datong River catchment, and our results are consistent with other studies proposing that when interpreting the weathering rate in the environment, there is an inseparable relationship between the chemical weathering rate and discharge (Hren et al., 2007; Noh et al., 2009; Maher et al., 2010), but no obvious effect by temperature (Huh, 2003; Riebe et al., 2004; Hagedorn and Cartwright, 2009).

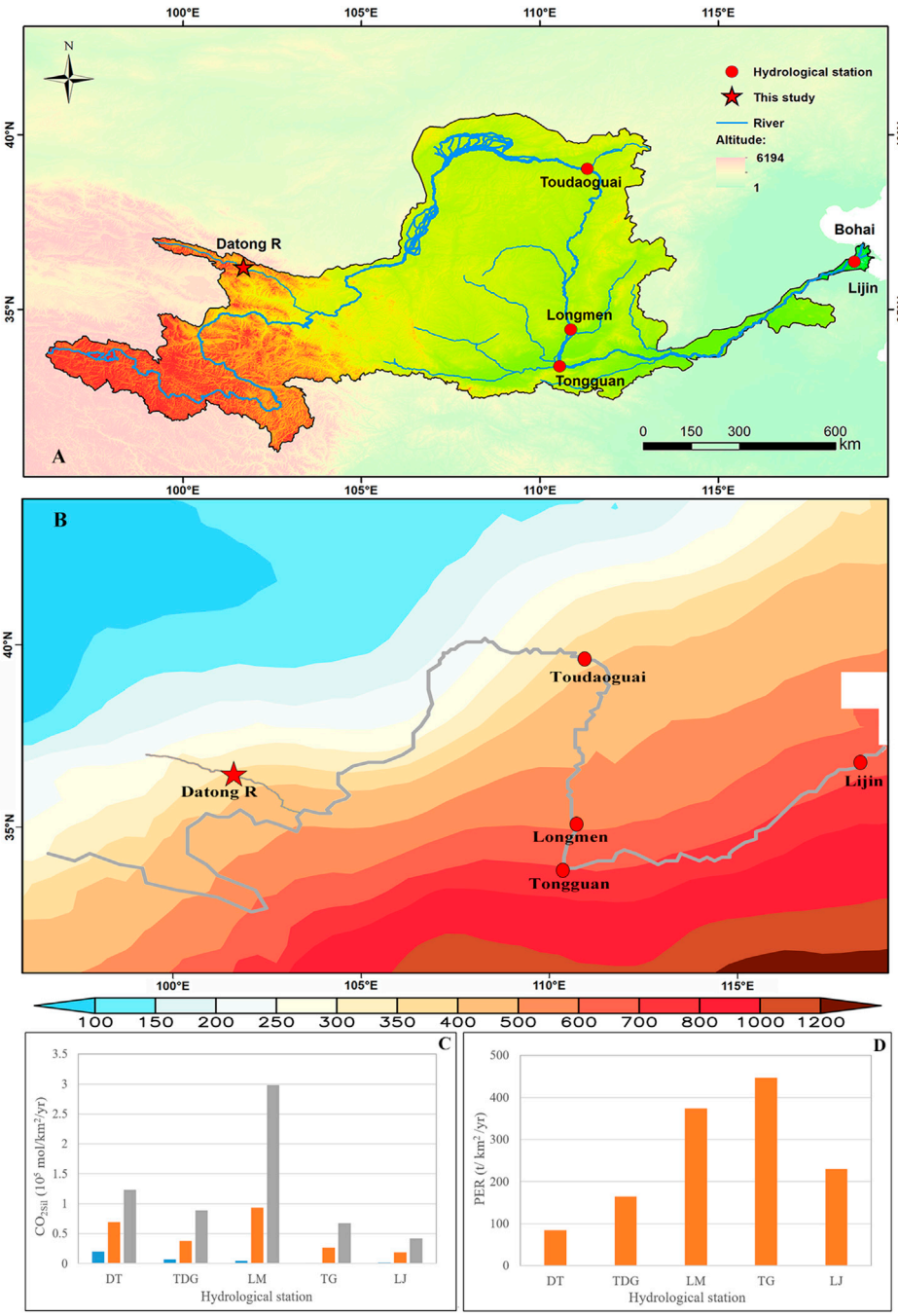

FIGURE 10 | Differences in chemical weathering among stations in the Yellow River basin. The $ØCO_{2sil}$ overall decreases from the upstream to the downstream of the Yellow River in **(C)**, whereas the physical erosion rate (PER) shows an increase trend in **(D)**. The Datong data (DT) come from this study, the Longmen data (LM) come from Zhang et al. (2015), the Toudaoguai (TDG), Tongguan (TG), and Lijin (LJ) data come from Ran et al. (2015). Study areas in this study and the compiled data are shown in **(A)**. The monthly average precipitation of the Yellow River basin from 2000 to 2020 is shown in **(B)**.

5.4 Weathering Differences From the Upper to Lower Reaches of the Yellow River Basin

The huge Yellow River basin spans contrasting tectonics, climate, vegetation, and lithology settings, which may lead to significant changes in the weathering process from the upstream to the downstream. Fan et al. (2014) reported that the CO_2 consumption rate of silicate in the upstream of the Yellow River was 0.14×10^5 mol/km^2/yr, lower than 0.69×10^5 mol/km^2/yr of the Datong River catchment calculated by precise weekly data. In the midstream to lower reaches of the Yellow River, the estimated

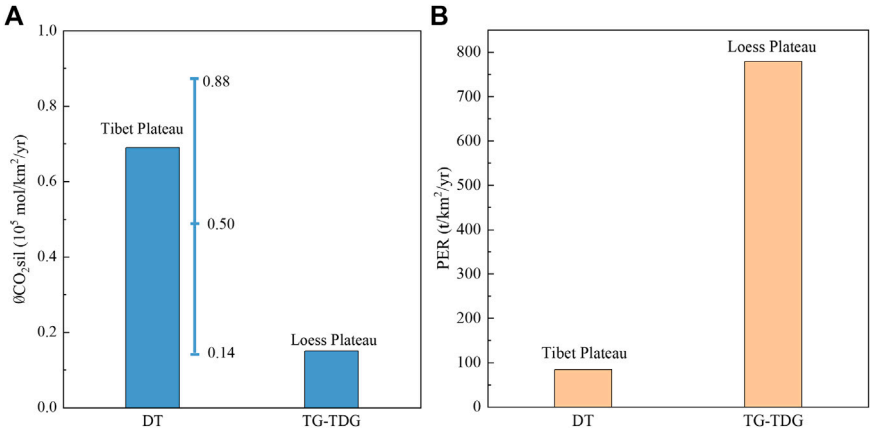

FIGURE 11 | Differences in **(A)** weathering and **(B)** erosion rates between the Tibet Plateau and Loess Plateau. The $ØCO_2$sil (0.69×10^5 mol/km^2/yr) calculated by the time-series data of the Datong River (DT) is within the range of spatial data ($0.14–0.88 \times 10^5$ mol/km^2/yr) at upper reaches of the Yellow River. The maximum value of the $ØCO_2$sil in the Tibet Plateau is 0.88 (at Lanzhou from Wu et al., 2005), the minimum value (at Tao River from Wu et al., 2005) is 0.14, and the average value is 0.50; the Loess Plateau data from Tongguan to Toudaoguai (TG-TDG) come from Ran et al. (2015). The physical erosion rate (PER) is estimated by suspended sediment data during 2013 from local hydrological stations.

$ØCO_{2sil}$ show significant differences by different studies, ranging from 0.18 to 0.99×10^5 mol/km^2/yr, excluding an extremely high value of 5.62×10^5 mol/km^2/yr (Fan et al., 2014; Ran et al., 2015; Zhang et al., 2015; Jia et al., 2021). We attributed this to different sampling strategies and calculation methods.

To comprehensively explore the accurate chemical weathering differences in different parts of the entire Yellow River basin, we therefore focus on the time-series sampling data (weekly or monthly) at the upstream (Datong River), midstream (Toudaoguai, Longmen, and Tongguan), and downstream (Lijin) (**Figure 10A**). An important point is that the $ØCO_{2sil}$ in each site varies in several orders of magnitudes, indicating that estimating the $ØCO_2$ by using one-time sampling at flood or dry seasons would introduce large uncertainties. It is also interesting to find that the overall trend of $ØCO_2$ decreases from the upstream to the downstream (**Figure 10B**). In contrast, the physical erosion rate (PER) increases dramatically from the upstream to the midstream and then declines at the downstream (**Figure 10C**). The most remarkable increase is between the midstream Toudaoguai and Tongguan, where the Yellow River drains the Chinese Loess Plateau.

In order to in-depth compare the weathering differences between the tectonically active Tibetan Plateau and the erodible Loess Plateau (**Figure 11**), we calculated the $ØCO_{2sil}$ between the Toudaoguai and Tongguan section (TDG-TG) of the Yellow River, where Loess weathering dominates the surficial weathering processes. The results show that $ØCO_{2sil}$ in the Datong River draining the Tibetan Plateau is 4.5 times higher than the Loess Plateau (**Figure 11A**). However, the PER is 9.5 times lower (**Figure 11B**). These results suggest that physical erosion is not a major factor controlling the weathering rates in the Yellow River basin. Given that the runoff in the Datong River (293 mm/yr in 2017) is much higher than the TDG-TG (53 mm/yr in 2013), showing a 5.5 times higher values, and very similar with the 4.5 times higher $ØCO_{2sil}$. We therefore propose that the runoff exerts a central role in silicate weathering and atmospheric CO_2 drawdown in the Yellow River basin.

6 CONCLUSION

A high frequency sampling (weekly) was conducted in the Datong River, through a whole hydrological year in 2017 to explore the chemical weathering processes in the upstream of the Yellow River draining the Tibetan Plateau. Our results show significantly seasonal changes of major ions, with lower concentrations in the monsoon period owing to the dilution effect by precipitation, and higher in the dry season. The largest contribution to the river solute in the Datong River was from carbonate weathering (46.07 ± 1.4%), while contribution from silicate weathering is minor (9.21 ± 1.57%). The $ØCO_{2sil}$ was 0.69×10^5 mol/km^2/yr in the upper reaches of the Yellow River at the Datong catchment. Comparing the middle and lower reaches, the silicate weathering and $ØCO_{2sil}$ show an overall decline trend by using five sets of weekly datasets, whereas the PER shows an increased trend. Finally, a comparison between the Yellow River draining the upstream Tibetan Plateau and the midstream Loess Plateau show 4.5 times higher $ØCO_{2sil}$ but 9.5 times lower PER. Together with annual runoff data, we propose that the runoff, rather than erosion, plays a central role on chemical weathering in the huge Yellow River basin.

DATA AVAILABILITY STATEMENT

The original contributions presented in the study are included in the article; further inquiries can be directed to the corresponding authors.

AUTHOR CONTRIBUTIONS

FZ designed and managed the project. LY and FZ wrote the manuscript. All authors contributed to the discussion and data interpretation.

FUNDING

This work was supported by the Strategic Priority Research Program of Chinese Academy of Sciences (XDB 40020502), the Youth Innovation Promotion Association of CAS (E029070299), the National Natural Science Foundation of China (41403111), and the Cultivating Foundation of the State Key Laboratory of Loess and Quaternary Geology (SKLLQG0923).

ACKNOWLEDGMENTS

We are very thankful to Y. Shi, Z. Ma, and Y. Li for help in sample collection and laboratory assistance. We are grateful to Y. Wei at Nanjing University and Y. Cao and M. Q. Liang at Hubei University for their kind help on laboratory work.

REFERENCES

Berner, R. A. (2001). GEOCARB III: A Revised Model of Atmospheric CO_2 over Phanerozoic Time. *Am. J. Sci.* 301 (4), 182–204. doi:10.2475/ajs.301.2.182

Bickle, M. J., Bunbury, J., Chapman, H. J., Harris, N. B. W., Fairchild, I. J., and Ahmad, T. (2003). Fluxes of Sr into the Headwaters of the Ganges. *Geochimica Cosmochimica Acta* 67 (14), 2567–2584. doi:10.1016/S0016-7037(03)00029-2

Bickle, M. J., Chapman, H. J., Tipper, E., Galy, A., De La Rocha, C. L., and Ahmad, T. (2018). Chemical Weathering Outputs from the Flood Plain of the Ganga. *Geochimica Cosmochimica Acta* 225, 146–175. doi:10.1016/j.gca.2018.01.003

Caves, J. K., Jost, A. B., Lau, K. V., and Maher, K. (2016). Cenozoic Carbon Cycle Imbalances and a Variable Weathering Feedback. *Earth Planet. Sci. Lett.* 450, 152–163. doi:10.1016/j.epsl.2016.06.035

Caves Rugenstein, J. K., Ibarra, D. E., von Blanckenburg, F., and Friedhelm, B. (2019). Neogene Cooling Driven by Land Surface Reactivity rather Than Increased Weathering Fluxes. *Nature* 571 (7763), 99–102. doi:10.3929/ethz-b-000338022

Chai, N., Yi, X., Xiao, J., Liu, T., Liu, Y., Deng, L., et al. (2021). Spatiotemporal Variations, Sources, Water Quality and Health Risk Assessment of Trace Elements in the Fen River. *Sci. Total Environ.* 757, 143882. doi:10.1016/j.scitotenv.2020.143882

Clift, P. D., and Jonell, T. N. (2021). Himalayan-Tibetan Erosion Is Not the Cause of Neogene Global Cooling. *Geophys Res. Lett.* 48 (8), e2020GL087742. doi:10.1029/2020GL087742

Dessert, C., Dupré, B., Gaillardet, J., François, L. M., Allègre, C. J., and Allègre., C. J. (2003). Basalt Weathering Laws and the Impact of Basalt Weathering on the Global Carbon Cycle. *Chem. Geol.* 202 (3), 257–273. doi:10.1016/j.chemgeo.2002.10.001

Dixon, J. L., Heimsath, A. M., and Amundson, R. (2009). The Critical Role of Climate and Saprolite Weathering in Landscape Evolution. *Earth Surf. Process. Landforms* 34 (11), 1507–1521. doi:10.1002/esp.1836

Dupré, B., Dessert, C., Oliva, P., Goddéris, Y., Viers, J., François, L., et al. (2003). Rivers, Chemical Weathering and Earth's Climate. *Comptes Rendus Geosci.* 335 (16), 1141–1160. doi:10.1016/j.crte.2003.09.015

Fan, B.-L., Zhao, Z.-Q., Tao, F.-X., Liu, B.-J., Tao, Z.-H., Gao, S., et al. (2014). Characteristics of Carbonate, Evaporite and Silicate Weathering in Huanghe River Basin: A Comparison Among the Upstream, Midstream and Downstream. *J. Asian Earth Sci.* 96, 17–26. doi:10.1016/j.jseaes.2014.09.005

Gaillardet, J., Dupré, B., Louvat, P., and Allegre, C. J. (1999). Global Silicate Weathering and CO_2 Consumption Rates Deduced from the Chemistry of Large Rivers. *Chem. Geol.* 159 (1-4), 3–30. doi:10.1016/S0009-2541(99)00031-5

Gaillardet, J., Calmels, D., Romero-Mujalli, G., Zakharova, E., and Hartmann, J. (2019). Global Climate Control on Carbonate Weathering Intensity. *Chem. Geol.* 527, 118762. doi:10.1016/j.chemgeo.2018.05.009

Gaillardet, J., and Galy, A. (2008). Himalaya--Carbon Sink or Source? *Science* 320 (5884), 1727–1728. doi:10.1126/science.1159279

Goldsmith, S. T., Carey, A. E., Johnson, B. M., Welch, S. A., Lyons, W. B., Mcdowell, W. H., et al. (2010). Stream Geochemistry, Chemical Weathering and CO_2 Consumption Potential of Andesitic Terrains, Dominica, Lesser Antilles. *Geochimica Cosmochimica Acta* 74 (1), 85–103. doi:10.1016/j.gca.2009.10.009

Grosbois, C., Négrel, P., Fouillac, C., and Grimaud, D. (2000). Dissolved Load of the Loire River: Chemical and Isotopic Characterization. *Chem. Geol.* 170 (1-4), 179–201. doi:10.1016/S0009-2541(99)00247-8

Hagedorn, B., and Cartwright, I. (2009). Climatic and Lithologic Controls on the Temporal and Spatial Variability of CO_2 Consumption via Chemical Weathering: An Example from the Australian Victorian Alps. *Chem. Geol.* 260 (3-4), 234–253. doi:10.1016/j.chemgeo.2008.12.019

Hren, M. T., Chamberlain, C. P., Hilley, G. E., Blisniuk, P. M., and Bookhagen, B. (2007). Major Ion Chemistry of the Yarlung Tsangpo-Brahmaputra River: Chemical Weathering, Erosion, and CO_2 Consumption in the Southern Tibetan Plateau and Eastern Syntaxis of the Himalaya. *Geochimica Cosmochimica Acta* 71 (12), 2907–2935. doi:10.1016/j.gca.2007.03.021

Huh, Y. (2003). Chemical Weathering and Climate - a Global Experiment: A Review. *Geosci. J.* 7 (3), 277–288. doi:10.1007/BF02910294

Jia, H., Qu, W., Ren, W., and Qian, H. (2021). Impacts of Chemical Weathering and Human Perturbations on Dissolved Loads of the Wei River, the Yellow River Catchment. *J. Hydrology* 603, 126950. doi:10.1016/j.jhydrol.2021.126950

Jiang, H., Liu, W., Xu, Z., Zhou, X., Zheng, Z., Zhao, T., et al. (2018). Chemical Weathering of Small Catchments on the Southeastern Tibetan Plateau I: Water Sources, Solute Sources and Weathering Rates. *Chem. Geol.* 500, 159–174. doi:10.1016/j.chemgeo.2018.09.030

Jin, Z., You, C.-F., Yu, J., Wu, L., Zhang, F., and Liu, H.-C. (2011). Seasonal Contributions of Catchment Weathering and Eolian Dust to River Water Chemistry, Northeastern Tibetan Plateau: Chemical and Sr Isotopic Constraints. *J. Geophys. Res.* 116 (F4). doi:10.1029/2011JF002002)

Lenard, S. J. P., Lavé, J., France-Lanord, C., Aumaître, G., Bourlès, D. L., Keddadouche, K., et al. (2020). Steady Erosion Rates in the Himalayas through Late Cenozoic Climatic Changes. *Nat. Geosci.* 13 (6), 448–452. doi:10.1038/s41561-020-0585-2

Li, X., Ding, Y., Han, T., Sillanpää, M., Jing, Z., You, X., et al. (2020). Seasonal and Interannual Changes of River Chemistry in the Source Region of Yellow River, Tibetan Plateau. *Appl. Geochem.* 119, 104638. doi:10.1016/j.apgeochem.2020.104638

Li, S., Goldstein, S. L., and Raymo, M. E. (2021). Neogene Continental Denudation and the Beryllium Conundrum. *Proc. Natl. Acad. Sci. U.S.A.* 118 (42), e2026456118. doi:10.1073/pnas.2026456118

Liu, W., Jiang, H., Shi, C., Zhao, T., Liang, C., Hu, J., et al. (2016a). Chemical and Strontium Isotopic Characteristics of the Rivers Around the Badain Jaran Desert, Northwest China: Implication of River Solute Origin and Chemical Weathering. *Environ. Earth Sci.* 75 (15), 1–16. doi:10.1007/s12665-016-5910-0

Liu, W., Shi, C., Xu, Z., Zhao, T., Jiang, H., Liang, C., et al. (2016b). Water Geochemistry of the Qiantangjiang River, East China: Chemical Weathering and CO 2 Consumption in a Basin Affected by Severe Acid Deposition. *J. Asian Earth Sci.* 127: 246–256. doi:10.1016/j.jseaes.2016.06.010

Liu, W., Xu, Z., Sun, H., Zhao, T., Shi, C., and Liu, T. (2018). Geochemistry of the Dissolved Loads during High-Flow Season of Rivers in the Southeastern Coastal Region of China: Anthropogenic Impact on Chemical Weathering and Carbon Sequestration. *Biogeosciences* 15 (16), 4955–4971. doi:10.5194/bg-15-4955-2018

Maher, K. (2010). The Dependence of Chemical Weathering Rates on Fluid Residence Time. *Earth Planet. Sci. Lett.* 294 (1-2), 101–110. doi:10.1016/j.epsl.2010.03.010

Meybeck, M. (1979). Concentrations des eaux fluviales en elements majeuis et apports en solution awx oceans. *Rev. Geol. Dyn. Geogr. Phys.* 21, 215–246.

Milliman, J. D., and Farnsworth, K. L. (2011). "Human Activities and Their Impacts," in *River Discharge to the Coastal Ocean: A Global Synthesis*. Editors J. D. Milliman and K. L. Farnsworth, 115–164.

Millot, R., Gaillardet, J., Bernard, D., and Claude, J. A. (2002). The Global Control of Silicate Weathering Rates and the Coupling with Physical Erosion: New Insights from Rivers of the Canadian Shield. *Earth Planet. Sci. Lett.* 196 (1-2), 83–98. doi:10.1016/S0012-821X(01)00599-4

Millot, R., Gaillardet, J. é., Dupré, B., and Allègre, C. J. (2003). Northern Latitude Chemical Weathering Rates: Clues from the Mackenzie River Basin, Canada. *Geochimica Cosmochimica Acta* 67 (7), 1305–1329. doi:10.1016/S0016-7037(02)01207-3

Ming-hui, H., Stallard, R. F., and Edmond, J. M. (1982). Major Ion Chemistry of Some Large Chinese Rivers. *Nature* 298 (5874), 550–553. doi:10.1038/298550a0

Moon, S., Chamberlain, C. P., and Hilley, G. E. (2014). New Estimates of Silicate Weathering Rates and Their Uncertainties in Global Rivers. *Geochimica Cosmochimica Acta* 134, 257–274. doi:10.1016/j.gca.2014.02.033

Moon, S., Huh, Y., Qin, J., and van Pho, N. (2007). Chemical Weathering in the Hong (Red) River Basin: Rates of Silicate Weathering and Their Controlling Factors. *Geochimica Cosmochimica Acta* 71 (6), 1411–1430. doi:10.1016/j.gca.2006.12.004

Moquet, J.-S., Crave, A., Viers, J., Seyler, P., Armijos, E., Bourrel, L., et al. (2011). Chemical Weathering and Atmospheric/soil CO_2 Uptake in the Andean and Foreland Amazon Basins. *Chem. Geol.* 287 (1-2), 1–26. doi:10.1016/j.chemgeo.2011.01.005

Noh, H., Huh, Y., Qin, J., and Ellis, A. (2009). Chemical Weathering in the Three Rivers Region of Eastern Tibet. *Geochimica Cosmochimica Acta* 73 (7), 1857–1877. doi:10.1016/j.gca.2009.01.005

Oliva, P., Viers, J., and Dupré, B. (2003). Chemical Weathering in Granitic Environments. *Chem. Geol.* 202 (3-4), 225–256. doi:10.1016/j.chemgeo.2002.08.001

Qu, B., Zhang, Y., Kang, S., and Sillanpää, M. (2017). Water Chemistry of the Southern Tibetan Plateau: an Assessment of the Yarlung Tsangpo River Basin. *Environ. Earth Sci.* 76 (2), 74. doi:10.1007/s12665-017-6393-3

Qu, Y., Jin, Z., Wang, J., Wang, Y., Xiao, J., Gou, L. F., et al. (2020). The Sources and Seasonal Fluxes of Particulate Organic Carbon in the Yellow River. *Earth Surf. Process. Landforms* 45 (9), 2004–2019. doi:10.1002/esp.4861

Ran, L., Lu, X. X., Richey, J. E., Sun, H., Han, J., Yu, R., et al. (20152015). Long-term Spatial and Temporal Variation of CO₂ Partial Pressure in the Yellow River, China. *Biogeosciences* 12 (4), 921–932. doi:10.5194/bg-12-921-2015

Raymo, M. E., Ruddiman, W. F., and Froelich, P. N. (1988). Influence of Late Cenozoic Mountain Building on Ocean Geochemical Cycles. *Geol* 16 (7), 649–653. doi:10.1130/0091-7613(1988)016<0649:iolcmb>2.3.co;2

Raymo, M. E., and Ruddiman, W. F. (1992). Tectonic Forcing of Late Cenozoic Climate. *Nature* 359 (6391), 117–122. doi:10.1038/359117a0

Riebe, C. S., Kirchner, J. W., and Finkel, R. C. (2004). Erosional and Climatic Effects on Long-Term Chemical Weathering Rates in Granitic Landscapes Spanning Diverse Climate Regimes. *Earth Planet. Sci. Lett.* 224 (3), 547–562. doi:10.1016/j.epsl.2004.05.019

Roy, S., Gaillardet, J., and Allègre, C. J. (1999). Geochemistry of Dissolved and Suspended Loads of the Seine River, France: Anthropogenic Impact, Carbonate and Silicate Weathering. *Geochimica cosmochimica acta* 63 (9), 1277–1292. doi:10.1016/S0016-7037(99)00099-X

Si, W., and Rosenthal, Y. (2019). Reduced Continental Weathering and Marine Calcification Linked to Late Neogene Decline in Atmospheric CO_2. *Nat. Geosci.* 12 (10), 833–838. doi:10.1038/s41561-019-0450-3

Singh, S. K., Sarin, M. M., and France-Lanord, C. (2005). Chemical Erosion in the Eastern Himalaya: Major Ion Composition of the Brahmaputra and δ13C of Dissolved Inorganic Carbon. *Geochimica Cosmochimica Acta* 69 (14), 3573–3588. doi:10.1016/j.gca.2005.02.033

Tipper, E. T., Bickle, M. J., Galy, A., West, A. J., Pomiès, C., and Chapman, H. J. (2006). The Short Term Climatic Sensitivity of Carbonate and Silicate Weathering Fluxes: Insight from Seasonal Variations in River Chemistry. *Geochimica Cosmochimica Acta* 70 (11), 2737–2754. doi:10.1016/j.gca.2006.03.005

Tipper, E. T., Stevenson, E. I., Alcock, V., Knight, A. C. G., Baronas, J. J., Hilton, R. G., et al. (2021). Global Silicate Weathering Flux Overestimated Because of Sediment-Water Cation Exchange. *Proc. Natl. Acad. Sci. U.S.A.* 118 (1). doi:10.1073/pnas.2016430118

Torres, M. A., West, A. J., and Li, G. (2014). Sulphide Oxidation and Carbonate Dissolution as a Source of CO_2 over Geological Timescales. *Nature* 507 (7492), 346–349. doi:10.1038/nature13030

Wang, L., Zhang, L., Cai, W.-J., Wang, B., and Yu, Z. (2016). Consumption of Atmospheric CO_2 via Chemical Weathering in the Yellow River Basin: The Qinghai-Tibet Plateau Is the Main Contributor to the High Dissolved Inorganic Carbon in the Yellow River. *Chem. Geol.* 430, 34–44. doi:10.1016/j.chemgeo.2016.03.018

West, A., Galy, A., and Bickle, M. (2005). Tectonic and Climatic Controls on Silicate Weathering. *Earth Planet. Sci. Lett.* 235 (1-2), 211–228. doi:10.1016/j.epsl.2005.03.020

West, A. J. (2012). Thickness of the Chemical Weathering Zone and Implications for Erosional and Climatic Drivers of Weathering and for Carbon-Cycle Feedbacks. *Geology* 40 (9), 811–814. doi:10.1130/G33041.1

White, A. F., and Blum, A. E. (1995). Effects of Climate on Chemical_ Weathering in Watersheds. *Geochimica Cosmochimica Acta* 59 (9), 1729–1747. doi:10.1016/0016-7037(95)00078-E

Willenbring, J. K., and Von Blanckenburg, F. (2010). Long-term Stability of Global Erosion Rates and Weathering during Late-Cenozoic Cooling. *Nature* 465 (7295), 211–214. doi:10.1038/nature09044

Wu, L., Huh, Y., Qin, J., Du, G., and van Der Lee, S. (2005). Chemical Weathering in the Upper Huang He (Yellow River) Draining the Eastern Qinghai-Tibet Plateau. *Geochimica Cosmochimica Acta* 69 (22), 5279–5294. doi:10.1016/j.gca.2005.07.001

Yu, Z., Wu, G., Keys, L., Li, F., Yan, N., Qu, D., et al. (2019). Seasonal Variation of Chemical Weathering and its Controlling Factors in Two Alpine Catchments, Nam Co Basin, Central Tibetan Plateau. *J. Hydrology* 576, 381–395. doi:10.1016/j.jhydrol.2019.06.042

Zhang, J., Huang, W. W., Letolle, R., and Jusserand, C. (1995). Major Element Chemistry of the Huanghe (Yellow River), China-weathering Processes and Chemical Fluxes. *J. Hydrology* 168 (1-4), 173–203. doi:10.1016/0022-1694(94)02635-O

Zhang, F., Jin, Z., Li, F., Yu, J., and Xiao, J. (2013a). Controls on Seasonal Variations of Silicate Weathering and CO_2 Consumption in Two River Catchments on the NE Tibetan Plateau. *J. Asian Earth Sci.* 62, 547–560. doi:10.1016/j.jseaes.2012.11.004

Zhang, F., Jin, Z., Li, F., Yu, J., You, C.-F., and Zhou, L. (2013b). The Dominance of Loess Weathering on Water and Sediment Chemistry within the Daihai Lake Catchment, Northeastern Chinese Loess Plateau. *Appl. Geochem.* 35, 51–63. doi:10.1016/j.apgeochem.2013.05.013

Zhang, Q., Jin, Z., Zhang, F., and Xiao, J. (2015). Seasonal Variation in River Water Chemistry of the Middle Reaches of the Yellow River and its Controlling Factors. *J. Geochem. Explor.* 156, 101–113. doi:10.1016/j.gexplo.2015.05.008

Zhang, L.-L., Zhao, Z.-Q., Zhang, W., Tao, Z.-H., Huang, L., Yang, J.-X., et al. (2016). Characteristics of Water Chemistry and its Indication of Chemical Weathering in Jinshajiang, Lancangjiang and Nujiang Drainage Basins. *Environ. Earth Sci.* 75 (6), 1–18. doi:10.1007/s12665-015-5115-y

Zhang, X., Xu, Z., Liu, W., Moon, S., Zhao, T., Zhou, X., et al. (2019). Hydro-Geochemical and Sr Isotope Characteristics of the Yalong River Basin, Eastern Tibetan Plateau: Implications for Chemical Weathering and Controlling Factors. *Geochem. Geophys. Geosyst.* 20 (3), 1221–1239. doi:10.1029/2018GC007769

Zhong, J., Li, S.-l., Tao, F., Ding, H., and Liu, J. (2017). Impacts of Hydrologic Variations on Chemical Weathering and Solute Sources in the Min River Basin, Himalayan-Tibetan Region. *Environ. Sci. Pollut. Res.* 24 (23), 19126–19137. doi:10.1007/s11356-017-9584-2

Conflict of Interest: The authors declare that the research was conducted in the absence of any commercial or financial relationships that could be construed as a potential conflict of interest.

Publisher's Note: All claims expressed in this article are solely those of the authors and do not necessarily represent those of their affiliated organizations, or those of the publisher, the editors, and the reviewers. Any product that may be evaluated in this article, or claim that may be made by its manufacturer, is not guaranteed or endorsed by the publisher.